Physics of Transcendental Numbers Determines Star Distribution

Hartmut Müller

Rome, Italy.
E-mail: hm@interscalar.com

Transcendental ratios of physical quantities can provide stability in complex dynamic systems because they inhibit the occurrence of destabilizing resonance between the elements of the system. This approach leads to a fractal scalar field that affects any type of physical interaction. In this paper we verify the model claims on the frequency distribution of interstellar distances in the solar neighborhood.

Introduction

Since the beginning of the past century astronomers began to routinely measure stellar parallaxes. In 1957 this effort was formalized with the publication [1] of 915 stars within 20 pc. Various updates and extensions to larger distances produced what became the Catalogue of Nearby Stars (CNS), including 3803 stars within 25 pc [2] released in 1991. Hipparcos [3] increased the quantity and quality of the CNS content. In 1998 the CNS dataset went online and currently has 5835 entries, but it is no longer updated. The most recent update [4] of the CNS was to provide accurate coordinates taken from the Two Micron Sky Survey (2MASS) [5]. Finally, the Gaia Catalogue of Nearby Stars (GCNS) attempts to make a census of all stars in the solar neighborhood using the Gaia results [6]. In the GCNS, the solar neighborhood is defined as a sphere with a radius of 100 pc centered on the Sun.

In this paper, we will analyze the distribution of the number of stars in the solar neighborhood as function of their mutual distances. This approach is not heliocentric and does not deal with fixed reference points at all.

Conventional models expect an exponential increase of the cumulative number of stars with the distance from a fixed reference point, such as the Sun. As shown in [6], this actually appears to be the case.

We will show that the consideration of all possible pairs of stars within a given range of interstellar distances leads to the appearance of a stable scale-invariant pattern in the frequency distribution of the number of stars as function of the distance between them. This means that there are interstellar distances preferred by the majority of stars in the solar neighborhood. Furthermore, we will derive this scale-invariant pattern from a number theoretic approach.

Methods

In [7] we have shown that the difference between rational, irrational algebraic and transcendental numbers is not only a mathematical task, but it is also an essential aspect of stability in complex dynamic systems. For instance, integer frequency ratios provide resonance interaction that can destabilize a system [8]. Actually, it is transcendental numbers that define the preferred ratios of quantities which avoid destabilizing res-

onance interaction [9]. In this way, transcendental ratios of quantities sustain the lasting stability of periodic processes in complex dynamic systems. With reference to the evolution of a planetary system and its stability, we may therefore expect that the ratio of any two orbital periods should finally approximate a transcendental number.

Among all transcendental numbers, Euler's number $e = 2.71828\ldots$ is unique, because its real power function e^x coincides with its own derivatives. In the consequence, Euler's number allows inhibiting resonance interaction regarding any interacting periodic processes and their derivatives. Because of this unique property of Euler's number, complex dynamic systems tend to establish relations of quantities that coincide with values of the natural exponential function e^x for integer and rational exponents x.

Therefore, we expect that periodic processes in real systems prefer frequency ratios close to Euler's number and its rational powers. Consequently, the logarithms of their frequency ratios should be close to integer $0, \pm 1, \pm 2, \ldots$ or rational values $\pm 1/2, \pm 1/3, \pm 1/4, \ldots$ In [10] we exemplified our hypothesis in particle physics, astrophysics, cosmology, geophysics, biophysics and engineering.

Based on this hypothesis, we introduced a fractal model of matter [11] as a chain system of harmonic quantum oscillators and could show the evidence of this model for all known hadrons, mesons, leptons and bosons as well. In [12] we have shown that the set of stable eigenstates in such systems is fractal and can be described by finite continued fractions:

$$\mathcal{F}_{jk} = \ln(\omega_{jk}/\omega_{00}) = \langle n_{j0}; n_{j1}, n_{j2}, \ldots, n_{jk} \rangle \qquad (1)$$

where ω_{jk} is the set of angular eigenfrequencies and ω_{00} is the fundamental frequency of the set. The denominators are integer: $n_{j0}, n_{j1}, n_{j2}, \ldots, n_{jk} \in \mathbb{Z}$. The cardinality $j \in \mathbb{N}$ of the set and the number $k \in \mathbb{N}$ of layers are finite. In the canonical form, all numerators equal 1. We use angle brackets for continued fractions.

Any finite continued fraction represents a rational number [13]. Therefore, the ratios ω_{jk}/ω_{00} of eigenfrequencies are always irrational, because for rational exponents the natural exponential function is transcendental [14]. This circumstance provides for lasting stability of those eigenstates of a

chain system of harmonic oscillators because it prevents resonance interaction [15] between the elements of the system.

The distribution density of stable eigenstates reaches local maxima near reciprocal integers $\pm 1/2, \pm 1/3, \pm 1/4, \ldots$ that are attractor points (fig. 1) in the fractal set $\mathcal{F}_{jk}$ of natural logarithms. Integer logarithms $0, \pm 1, \pm 2, \ldots$ represent the most stable eigenstates (main attractors).

In the case of harmonic quantum oscillators, the continued fractions $\mathcal{F}_{jk}$ define not only fractal sets of natural angular frequencies ω_{jk}, angular accelerations $a_{jk} = c \cdot \omega_{jk}$, oscillation periods $\tau_{jk} = 1/\omega_{jk}$ and wavelengths $\lambda_{jk} = c/\omega_{jk}$ of the chain system, but also fractal sets of energies $E_{jk} = \hbar \cdot \omega_{jk}$ and masses $m_{jk} = E_{jk}/c^2$ which correspond with the eigenstates of the system. For this reason, we call the continued fraction $\mathcal{F}_{jk}$ the *Fundamental Fractal* of stable eigenstates in chain systems of harmonic quantum oscillators.

Fig. 1: The distribution of stable eigenvalues of $\mathcal{F}_{jk}$ for $k = 1$ (above) and for $k = 2$ (below) in the range $-1 \leqslant \mathcal{F}_{jk} \leqslant 1$.

The spatio-temporal projection of the Fundamental Fractal $\mathcal{F}_{jk}$ of stable eigenstates is a fractal scalar field of transcendental attractors, the *Fundamental Field* [16].

The connection between the spatial and temporal projections of the Fundamental Fractal is given by the speed of light $c = 299792458$ m/s. The constancy of c makes both projections isomorphic, so that there is no arithmetic or geometric difference. Only the units of measurement are different.

Figure 2 shows the linear 2D-projection $\exp(\mathcal{F}_{jk})$ of the first layer of the Fundamental Field

$$\mathcal{F}_{j1} = \langle n_{j0}; n_{j1} \rangle = n_{j0} + \frac{1}{n_{j1}}$$

in the interval $-1 < \mathcal{F}_{j1} < 1$. The upper part of figure 1 shows the same interval in the logarithmic representation. The Fundamental Field is topologically 3-dimensional, a fractal set of embedded spheric equipotential surfaces. The logarithmic potential difference defines a gradient directed to the center of the field that causes a central force of attraction. Because of the fractal logarithmic hyperbolic metric of the field, every equipotential surface is an attractor.

The Fundamental Field is of pure arithmetical origin, and there is no particular physical mechanism required as field source. It is all about transcendental ratios of frequencies [9] that inhibit destabilizing resonance. Therefore, we postulate the universality of the Fundamental Field that affects any type of physical interaction, regardless of its complexity.

In fact, scale relations in particle physics [11] and astrophysics [17] obey the same Fundamental Fractal (1), without any additional or particular settings. The proton-to-electron rest energy ratio approximates the first layer of the Fundamental Fractal that could explain their exceptional stability.
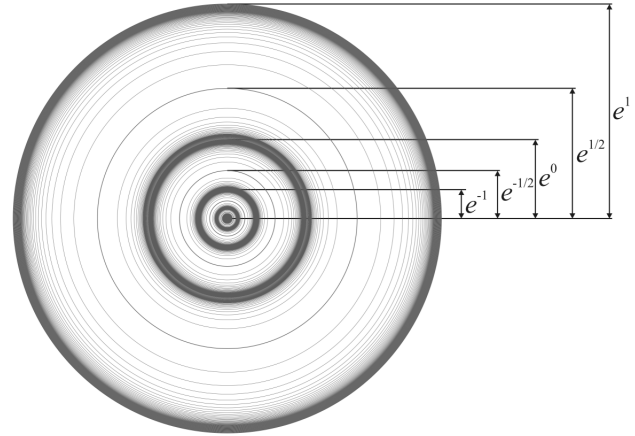

Fig. 2: The equipotential surfaces of the Fundamental Field in the linear 2D-projection for $k = 1$.

In fact, the life-spans of the proton and electron top everything that is measurable, exceeding 10^{29} years [18].

PROPERTY	ELECTRON	PROTON
$E = mc^2$	0.5109989461(31) MeV	938.2720813(58) MeV
$\omega = E/\hbar$	$7.76344 \cdot 10^{20}$ Hz	$1.42549 \cdot 10^{24}$ Hz
$\tau = 1/\omega$	$1.28809 \cdot 10^{-21}$ s	$7.01515 \cdot 10^{-25}$ s
$\lambda = c/\omega$	$3.86159 \cdot 10^{-13}$ m	$2.10309 \cdot 10^{-16}$ m

Table 1: The basic set of the physical properties of the electron and proton. Data from Particle Data Group [18]. Frequencies, oscillation periods and wavelengths are calculated.

The proton-to-electron ratio (tab. 1) approximates the seventh power of Euler's number and its square root:

$$\ln\left(\frac{\lambda_e}{\lambda_p}\right) = \ln\left(\frac{3.86159 \cdot 10^{-13}\,\text{m}}{2.10309 \cdot 10^{-16}\,\text{m}}\right) \simeq 7 + \frac{1}{2} = \langle 7; 2 \rangle$$

In the consequence of this potential difference of the proton relative to the electron, the scaling factor $\sqrt{e} = 1.64872\ldots$ connects attractors of proton stability with similar attractors of electron stability in alternating sequence. The following Diophantine equation describes the correspondence of proton calibrated attractors n_p with electron calibrated attractors n_e. Non considering the signature, only three pairs (n_p, n_e) of integers are solutions to this equation: (3, 6), (4, 4), (6, 3).

$$\frac{1}{n_p} + \frac{1}{n_e} = \frac{1}{2}$$

Figure 3 demonstrates this situation on the first layer of the Fundamental Fractal (1). Both, the attractors of proton and electron stability are represented at the first layer, so we can see clearly that among the integer or half, only the attractors $\pm 1/3, \pm 1/4$ and $\pm 1/6$ are common. In these attractors, proton

stability is supported by electron stability and vice versa, so we expect that they are preferred in real systems.
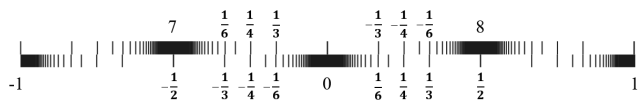

Fig. 3: The distribution of the attractors of proton (bottom) stability in the range $-1 < \mathcal{F} < 1$ of the attractors of electron (top) stability. Natural logarithmic representation.

These unique properties of the electron and proton predestine their physical characteristics as fundamental units. Table 1 shows the basic set of electron and proton units that can be considered as a fundamental metrology (c is the speed of light in a vacuum, $\hbar$ is the Planck constant). In [12] was shown that the fundamental metrology (tab. 1) is completely compatible with Planck units [19]. Originally proposed in 1899 by Max Planck, these units are also known as natural units, because the origin of their definition comes only from properties of nature and not from any human construct. Max Planck wrote [20] that these units, "regardless of any particular bodies or substances, retain their importance for all times and for all cultures, including alien and non-human, and can therefore be called natural units of measurement". Planck units reflect the characteristics of space-time.

We assume that scale invariance according to the Fundamental Fractal (1), which is calibrated to the physical properties of the proton and the electron, is a universal characteristic of organized matter and criterion of stability. This hypothesis we have called *Global Scaling* [10].

In this paper we will show that the distribution of interstellar distances in the solar neighborhood corresponds with the distribution of attractors in the Fundamental Field.

Results

In [21] we applied the Fundamental Fractal (1) to macroscopic scales interpreting gravity as attractor effect of its stable eigenstates. Indeed, the orbital and rotational periods of planets, planetoids and large moons of the solar system correspond with attractors of electron and proton stability [12]. This is valid also for the planets [10] of the systems Trappist 1 and Kepler 20. Planetary and lunar orbits [17] correspond with equipotential surfaces of the Fundamental Field.

Figure 4 shows the distribution of the number of exoplanets with orbital periods in the range 5 d $< T < 24$ d that corresponds with logarithms $59.2 < ln\,(T/2\pi\tau_e) < 60.8$ on the horizontal axis. According with table 1, τ_e is the electron angular oscillation period. The histogram contains data of 1430 exoplanets and shows clearly the maximum corresponding with the main attractor $\mathcal{F}\langle 60 \rangle$. Other maxima correspond with the attractors $\mathcal{F}\langle 59; 2 \rangle$ and $\mathcal{F}\langle 60; 2 \rangle$; even the subattractors $\mathcal{F}\langle 60; -4 \rangle$ and $\mathcal{F}\langle 60; 4 \rangle$ can be distinguished.

The histogram evidences that the majority of the 1430 exoplanets [22] prefer orbital periods close to 10–11 days cor-
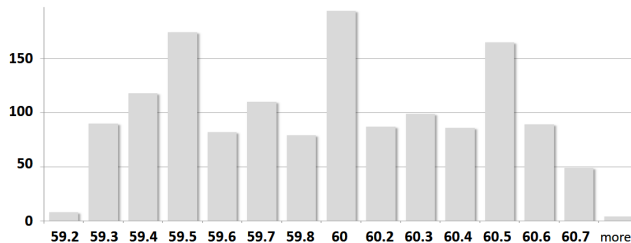

Fig. 4: The histogram shows the distribution of the number of exoplanets with orbital periods in the range 5 d $< T < 24$ d. The logarithms $ln\,(T/2\pi\tau_e)$ are on the horizontal axis. Corresponding with table 1, τ_e is the electron angular oscillation period. Data of 1430 exoplanets are taken from [22].

responding with the main attractor $\mathcal{F}\langle 60 \rangle$, as well as periods close to 6–7 days or close to 17–18 days corresponding with the attractors $\mathcal{F}\langle 59; 2 \rangle$ and $\mathcal{F}\langle 60; 2 \rangle$. Because of the logarithm 7+1/2 of the proton-to-electron ratio, the attractors $\mathcal{F}\langle 59; 2 \rangle$ and $\mathcal{F}\langle 60; 2 \rangle$ of *electron* stability are actually the main attractors $\mathcal{F}\langle 67 \rangle$ and $\mathcal{F}\langle 68 \rangle$ of *proton* stability.

Figure 5a shows the distribution of the number of stars as function of their distances R from the Sun up to 25 light-years that correspond with the logarithms $ln\,(R/\lambda_e) < 68.6$ on the horizontal axis. According with table 1, λ_e is the Compton wavelength of the electron. The histogram contains 192 distances and shows clearly the maxima corresponding with the attractors $\mathcal{F}\langle 67 \rangle$, $\mathcal{F}\langle 67; 2 \rangle$, $\mathcal{F}\langle 68 \rangle$ and $\mathcal{F}\langle 68; 2 \rangle$.

Knowing the right ascension, declination and distances of two stars from the Sun, it is not difficult to calculate the distance between them. In preparation of this paper, the mutual distances between the 192 best measured stars including Vega within a radius of 25 light-years around the Sun were calculated. The number of pairs of stars is given by the formula:

$$P = N(N - 1)/2$$

where N is the number of stars; P is the number of pairs. For 192 stars, we calculated $P = 18,336$ interstellar distances.

Figure 5b shows the distribution of the number of stars as function of their distances R from Sirius up to 33 light-years. Also this histogram shows clearly the maxima corresponding with the attractors $\mathcal{F}\langle 67 \rangle$, $\mathcal{F}\langle 67; 2 \rangle$, $\mathcal{F}\langle 68 \rangle$ and $\mathcal{F}\langle 68; 2 \rangle$. The same $\mathcal{F}$-pattern appears in the histograms of interstellar distances measured from Barnard's star (fig. 5b), Tau Ceti (fig. 5d) and other stars in the 25-light-years solar neighborhood. Only the expression of the $\mathcal{F}$-pattern differs in strength.

Conclusion

Standard models expecting an exponential increase of the cumulative number of stars with the distance from a fixed reference point, perhaps could interpret the local maxima in the histograms as anomalies evidencing that the solar neighborhood is still in transformation. Within our approach, on the contrary, the coincidence of the maxima with attractors of the Fundamental Field evidences that the solar neighborhood has
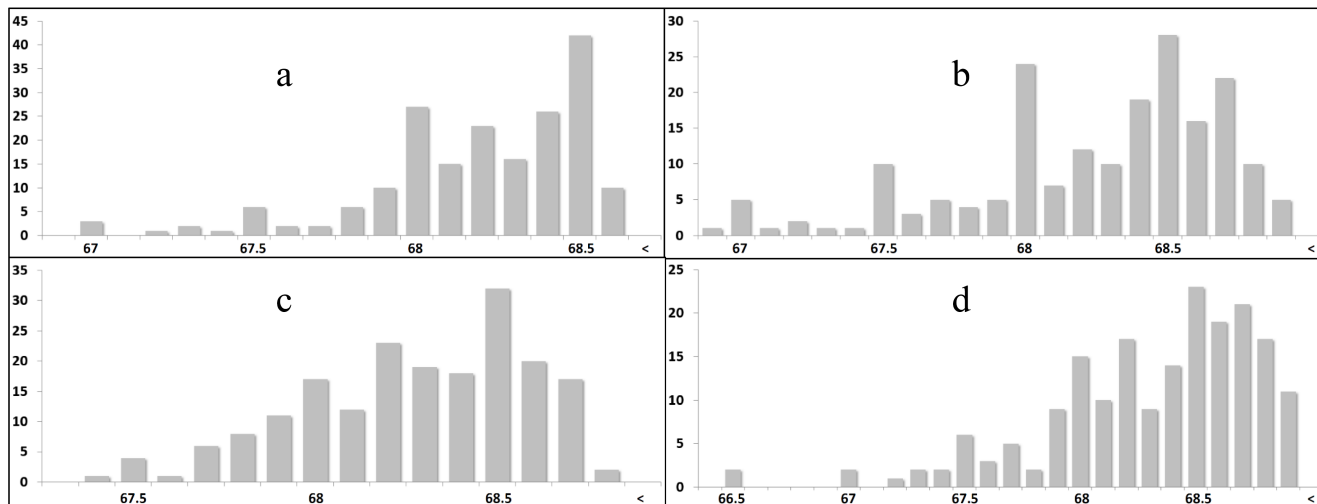
Fig. 5: The histogram shows the distribution of the number of stars in the solar neighborhood as function of their distances R from the Sun (a), Sirius (b), Barnard's star (c) and Tau Ceti (d). The logarithms $\ln (R/\lambda_e)$ are on the horizontal axis. Corresponding with table 1, λ_e is the Compton wavelength of the electron. Data of 192 stars are taken from [23].

already reached a certain level of stability. Moreover, we expect a continuous amplification of $\mathcal{F}$-patterns in histograms as trend of interstellar distances. Most likely, the appearance of patterns corresponding with the Fundamental Fractal (1) is a universal criterion of stability.

Since the Fundamental Fractal is of number theoretic origin, it determines the frequency distributions of interstellar distances as well as the wavelengths of elementary particles. Interscalar cosmology [10] bases on this approach.

Acknowledgements

References

1. Gliese W. Astronomisches Rechen-Institut Heidelberg Mitteilungen Serie A, 1957, v. 8, 1.

2. Gliese W., Jahreiß H. Preliminary Version of the Third Catalogue of Nearby Stars: The Astronomical Data Center CD-ROM. Selected Astronomical Catalogs, (1991).

3. Perryman M. A. C. The Hipparcos Catalogue. *Astron. Astrophys.*, 1997, v. 323, L49–L52.

4. Stauffer J. et al. *PASP*, 2010, v. 122, 885.

5. Skrutskie M. F. et al. *AJ*, 2006, v. 131, 1163.

6. Gaia Collaboration, Smart R. L. et al. Gaia Early Data Release 3: The Gaia Catalogue of Nearby Stars. arXiv:2012.02061v1 [astro-ph.SR] 3 Dec 2020.

7. Müller H. On the Cosmological Significance of Euler's Number. *Progress in Physics*, 2019, v. 15, 17–21.

8. Dombrowski K. Rational Numbers Distribution and Resonance. *Progress in Physics*, 2005, v. 1, no. 1, 65–67.

9. Müller H. The Physics of Transcendental Numbers. *Progress in Physics*, 2019, v. 15, 148–155.

10. Müller H. Global Scaling. The Fundamentals of Interscalar Cosmology. *New Heritage Publishers*, Brooklyn, New York, USA, ISBN 978-0-9981894-0-6, (2018).

11. Müller H. Fractal Scaling Models of Natural Oscillations in Chain Systems and the Mass Distribution of Particles. *Progress in Physics*, 2010, v. 6, 61–66.

12. Müller H. Scale-Invariant Models of Natural Oscillations in Chain Systems and their Cosmological Significance. *Progress in Physics*, 2017, v. 13, 187–197.

13. Khintchine A.Ya. Continued fractions. University of Chicago Press, Chicago, (1964).

14. Hilbert D. Über die Transcendenz der Zahlen e und π. *Mathematische Annalen*, 1893, v. 43, 216–219.

15. Panchelyuga V.A., Panchelyuga M. S. Resonance and Fractals on the Real Numbers Set. *Progress in Physics*, 2012, v. 8, no. 4, 48–53.

16. Müller H. Quantum Gravity Aspects of Global Scaling and the Seismic Profile of the Earth. *Progress in Physics*, 2018, vol. 14, 41–45.

17. Müller H. Global Scaling of Planetary Systems. *Progress in Physics*, 2018, v. 14, 99–105.

18. Tanabashi M. et al. (Particle Data Group), Phys. Rev. D 98, 030001 (2018), www.pdg.lbl.gov

19. Astrophysical constants. Particle Data Group, pdg.lbl.gov

20. Planck M. Über Irreversible Strahlungsvorgänge. *Sitzungsbericht der Königlich Preußischen Akademie der Wissenschaften*, 1899, v. 1, 479–480.

21. Müller H. Gravity as Attractor Effect of Stability Nodes in Chain Systems of Harmonic Quantum Oscillators. *Progress in Physics*, 2018, v. 14, 19–23.

22. Catalog of Exoplanets. Observatoire de Paris, http://exoplanet.eu/

23. Gaia EDR3, https://www.cosmos.esa.int/web/gaia/earlydr3